Received: 17 September 2020 | Revised: 29 October 2020 | Accepted: 2 November 2020

DOI: 10.1111/joa.13364

Journal of Anatomy ANATOMICAL SOCIETY WILEY

ORIGINAL PAPER

Head adaptation for sound production and feeding strategy in dolphins (Odontoceti: Delphinida)

Guilherme Frainer[1] | Stefan Huggenberger[2] | Ignacio B. Moreno[1,3] | Anders Galatius[4]

[1]Programa de Pós-Graduação em Biologia Animal, Departamento de Zoologia, Universidade Federal do Rio Grande do Sul, Porto Alegre, Brazil

[2]University of Witten/Herdecke gGmbH, Witten, Germany

[3]Centro de Estudos Costeiros, Limnológicos e Marinhos (CECLIMAR/CLN/UFRGS), Universidade Federal do Rio Grande do Sul, Imbé, Brazil

[4]Marine Mammal Research, Department of Bioscience, Aarhus University, Roskilde, Denmark

Correspondence
Guilherme Frainer, Programa de Pós-Graduação em Biologia Animal, Departamento de Zoologia, Universidade Federal do Rio Grande do Sul, Porto Alegre, Brazil.
Email: gui.frainer@gmail.com

Funding information
Conselho Nacional de Desenvolvimento Científico e Tecnológico, Grant/Award Number: 201709/2015-5; Coordenação de Aperfeiçoamento de Pessoal de Nível Superior; Society for Marine Mammalogy

Abstract

Head morphology in toothed whales evolved under selective pressures on feeding strategy and sound production. The postnatal development of the skull (n = 207) and mandible (n = 219) of six Delphinida species which differ in feeding strategy but exhibit similar sound emission patterns, including two narrow-band high-frequency species, were investigated through 3D morphometrics. Morphological changes throughout ontogeny were demonstrated based on the main source of variation (i.e., prediction lines) and the common allometric component. Multivariate trajectory analysis with pairwise comparisons between all species was performed to evaluate specific differences on the postnatal development of skulls and mandibles. Changes in the rostrum formation contributed to the variation (skull: 49%; mandible: 90%) of the entire data set and might not only reflect the feeding strategy adopted by each lineage but also represents an adaptation for sound production and reception. As an important structure for directionality of sound emissions, this may increase directionality in raptorial feeders. Phylogenetic generalized least squares analyses indicated that shape of the anterior portion of the skull is strongly dependent on phylogeny and might not only reflect feeding mode, but also morphological adaptations for sound production, particularly in raptorial species. Thus, postnatal development seems to represent a crucial stage for biosonar maturation in some raptorial species such as *Pontoporia blainvillei* and *Sousa plumbea*. The ontogeny of their main tool for navigation and hunting might reflect their natural history peculiarities and thus potentially define their main vulnerabilities to anthropogenic changes in the environment.

KEYWORDS
3D morphometrics, echolocation, feeding strategy, macroevolution, ontogeny, toothed whales

1 | INTRODUCTION

Toothed whales (Cetartiodactyla: Odontoceti) are remarkable for the evolution of an extremely hydrodynamic cetacean body (Fish, 2002; Thewissen et al., 2006) and an echolocation-based system for navigation and hunting (Geisler et al., 2014; Norris et al., 1961). Most dolphins of the infraorder Delphinida, particularly delphinids, produce broad-band sounds (BB) for echolocation (Au, 2000). However, some lineages have independently evolved the ability to produce highly directional (Wei et al., 2019) narrow-band high frequency (NBHF) sounds (Kyhn et al., 2010) for echolocation as observed in *Kogia* species, *Pontoporia blainvillei*, Phocoenidae and *Cephalorhynchus* species. Investigation of the evolution of the sound generating structures in Delphinida has revealed that species with highly directional signals

convergently developed distinct head features to achieve increased directionality (Frainer et al., 2019a). However, feeding strategy might also determine sound emission patterns as not only preferred preys might differ between strategies (McCurry et al., 2017), but emitted sounds may also be affected by distinct rostrum morphologies adapted for suction or raptorial feeding (Song et al., 2016; Werth, 2006).

Sound production for echolocation in dolphins is assumed to occur in the right portion of the epicranial complex (Madsen et al., 2013; Ridgway et al., 2015), precisely at the right monkey-lip dorsal bursae (MLDB) complex (Frainer et al., 2019a; Huggenberger et al., 2009). Echolocation sounds are modulated by their interaction with the skull, dense connective tissue theca and the vestibular air sacs (Wei et al., 2017) at the epicranial complex. Sounds are then collimated through the right branch of the melon (Frainer et al., 2019a; Wei et al., 2017) and can, additionally, be modulated by the rostrum which is supposed to reflect the sound while decreasing the frequency emitted (Song et al., 2016). The sound is reflected by objects in the environment and echoes are perceived via intramandibular fat bodies at the mandibular window of the lower jaw – by the tympano-periotic complex including the middle and inner ears (Bullock et al., 1968; Norris, 1968).

Toothed whale biosonar frequency evolution was primarily driven by selection for a narrow acoustic field of view which facilitates long-range prey detection (Jensen et al., 2018). Directionality in dolphin echolocation sounds plays a role in target detection as it tends to increase source level in the forward direction where click energy presents its elevated centre frequency. Thus, the range for target detection increases while reflections from the periphery are reduced (Finneran et al., 2014; Jensen et al., 2009; Koblitz et al., 2012).

The evolution of highly directional sound emissions in dolphins has strong influence on their natural history including the basics as environment perception and foraging. In this study, we used 3D geometric morphometrics to investigate skull and mandible transformation and variation throughout the postnatal development of six species within the infraorder Delphinida, which differ in feeding strategy, but exhibit similar sound emission patterns, including two NBHF species. Additionally, a macroevolutionary approach was employed to demonstrate sound production patterns in toothed whales and their relation to rostrum morphology and feeding strategy. Comparative studies on skull and mandible morphology might be helpful to understand the distinct pathways (ontogenies) some lineages might have followed to achieve similar and typical sonar properties, as well as their implications on life history and under the influence of changing environment.

2 | MATERIALS AND METHODS

2.1 | Samples

The specimens analyzed here are housed in the collections of the Natural Sciences Museum of the Federal University of Rio Grande do Sul (MUCIN/UFRGS), *Grupo de Estudos de Mamíferos Aquáticos do Rio Grande do Sul* (GEMARS), Natural History Museum of Copenhagen (NHMC) and Port Elizabeth Museum at Bayworld (PEM). Skulls (n = 207) and right mandibles (n = 219) from neonates to adults were selected to elucidate an ontogenetic series for each species, including: 34 skulls and 32 mandibles of the Franciscana dolphin, *Pontoporia blainvillei* (Gervais & d'Orbigny, 1844); 63 skulls and 69 mandibles of the harbour porpise, *Phocoena phocoena* (Linnaeus, 1758); 26 skulls and 30 mandibles of white-beaked dolphin, *Lagenorhynchus albirostris* (Gray, 1846); 44 skulls and 49 mandibles of the humpback dolphin, *Sousa plumbea* (G. Cuvier, 1829); 20 skulls and 16 mandibles of the common bottlenose dolphin, *Tursiops truncatus* (Montagu, 1821); and 20 skulls and 19 mandibles of the Lahille´s bottlenose dolphin, *Tursiops gephyreus* Lahille, 1908. In this study, the general shape transformation throughout the ontogeny was taken into account.

2.2 | Shape digitalization

Skull and mandible shapes were assessed using 3D geometric morphometrics. Three-dimensional coordinates of 63 landmarks for the skull (adapted from Galatius and Gol'din, 2011, Galatius & Goodall, 2016) (File S1A) and eight landmarks for the right mandible (adapted from Barroso et al., 2012) (File S1B) were registered using a Microscribe® 3D digitizer (Table 1). Landmarks are illustrated in File S2. Terminology follows Mead and Fordyce (2009) for the skull and mandible.

2.3 | Statistical analysis

All subsequent analyses, including the next section, were performed in R (R Core Team, 2020). Missing landmarks were estimated through the thin-plate spline method (*estimate.missing* function, see below) (Gunz et al., 2009). Then, a generalized Procrustes superimposition (*gpagen* function, see below) (Rohlf & Slice, 1990) on the three-dimensional landmarks was performed and the centroid size values (CS) were retained. The mean shapes for the skull and mandible were assessed through the *mshape* function (see below) to characterize the general arrangement of the landmarks. A linear model was performed to quantify the relative amount of shape variation in relation to variation of the centroid size (CS) (*procD.lm* function, see below) (Bookstein, 1991). The fitted linear model was then used to calculate standardized shape scores at different values of CS. Thus, prediction lines for the skull and mandible development for each species were created by plotting the first principal component of "predicted" values from the linear model with size (Adams & Nistri, 2010).

Since odontocetes exhibit a linear ontogeny (Galatius, 2010) a vector, the common allometric component (CAC) of the shape data was calculated as the estimation of the average allometric trend for group-mean centred data. Vectors describing directionalities of residual variation, in order of decreasing importance, were defined through a principal component analysis (*gm.prcomp* function, see below) on the residuals of the CAC. These vectors

TABLE 1 Three-dimensional coordinates were obtained from 63 landmarks on the skull (1–63) and eight landmarks on the right mandible (A–H). Additionally, the contribution of each landmark to the PCA for the fitted values from the regression model (i.e., RSC's) for the skull and mandible datasets are presented

ID	Landmark description	Contrib. to RSC1 (%)	Contrib. to RSC2 (%)
1	Anterior tip of right premaxillary	**49.06**	4.30
2	The caudalmost alveoli (right)	1.36	0.63
3	The caudalmost alveoli (left)	1.15	1.07
4	Anterior point of lacrimal (right)	0.83	1.34
5	Anterior point of lacrimal (left)	0.95	0.72
6	Anterior point of frontal (right)	1.58	4.08
7	Anterior point of frontal (left)	1.66	2.82
8	Tip of the antorbital process (right)	0.92	**4.77**
9	Tip of the antorbital process (left)	0.94	3.29
10	Anterior base of the postorbital process of the frontal (right)	1.93	1.54
11	Anterior base of the postorbital process of the frontal (left)	1.76	1.20
12	Ventral point of the postorbital process of the frontal (right)	1.54	2.04
13	Ventral point of the postorbital process of the frontal (left)	1.40	1.51
14	Posterior base of the postorbital process of the frontal (right)	2.31	0.18
15	Posterior base of the postorbital process of the frontal (left)	2.25	0.53
16	Posterior margin of anterior dorsal infraorbital foramen (right)	0.35	1.15
17	Posterior margin of anterior dorsal infraorbital foramen (left)	0.30	0.53
18	Anterior margin of the posterior dorsal infraorbital foramen (right)	0.33	0.47
19	Anterior margin of the posterior dorsal infraorbital foramen (left)	0.26	0.22
20	Posterior tip of premaxillary (right)	0.81	**6.62**
21	Posterior tip of premaxillary (left)	0.72	2.13
22	Nasal septum at the anterior end of the nasal apertures	0.63	0.04
23	Intersection of the ethmoid with the suture between the nasal bones	0.30	4.17
24	Intersection of the interparietal with the suture between the nasal bones	0.53	0.65
25	Ventral tip of the nasal (right)	0.22	2.03
26	Ventral tip of the nasal (left)	0.22	2.28
27	Dorsal tip of the nasal (right)	0.80	1.66
28	Dorsal tip of the nasal (left)	0.76	1.21
29	Anteriormost point of the sutures between the frontal and interparietal bones	**2.33**	0.20
30	Dorsal tip of occipital condyle (right)	0.70	2.45
31	Dorsal tip of occipital condyle (left)	0.83	2.48

(Continues)

(Continues)

TABLE 1 (Continued)

ID	Landmark description	Contrib. to RSC1 (%)	Contrib. to RSC2 (%)
32	Medial point of the intercondyloid notch of the basioccipital in ventral aspect	0.88	2.74
33	Angle of the frontal–parietal suture at the lateral margin of the bones (right)	1.94	1.36
34	Angle of the frontal–parietal suture at the lateral margin of the bones (left)	1.58	0.94
35	Junction of supraoccipital, exoccipital and parietal (right)	1.16	2.66
36	Junction of supraoccipital, exoccipital and parietal (left)	1.07	2.39
37	Junction of exoccipital, parietal and squamosal (right)	0.97	1.41
38	Junction of exoccipital, parietal and squamosal (left)	0.86	1.28
39	Anterior tip of exoccipital at the base of the zygomatic process of the squamosal (right)	0.55	2.67
40	Anterior tip of exoccipital at the base of the zygomatic process of the squamosal (left)	0.49	3.04
41	Junction of the parietal, frontal and sphenoid (right)	0.31	0.60
42	Junction of the parietal, frontal and sphenoid (left)	0.25	0.63
43	Dorsal tip of the squamosal (right)	0.65	2.35
44	Dorsal tip of the squamosal (left)	0.58	1.41
45	Tip of the zygomatic process of the squamosal (right)	1.53	1.20
46	Tip of the zygomatic process of the squamosal (left)	1.34	1.24
47	Suture of pterygoid and basioccipital at the lateral margin of the bones (right)	0.31	0.32
48	Suture of pterygoid and basioccipital at the lateral margin of the bones (left)	0.29	0.27
49	Deep point of the Eustachian notch (right)	0.25	1.33
50	Deep point of the Eustachian notch (left)	0.25	1.56
51	Posterior tip of the pterygoid hamulus (right)	0.18	0.20
52	Posterior tip of the pterygoid hamulus (left)	0.18	0.33
53	Posterior end of pterygoid–palatine suture (right)	0.12	0.62
54	Posterior end of pterygoid–palatine suture (left)	0.14	0.61
55	Posterior tip of right palatine	0.03	1.95
56	Anterior margin of the ventral infraorbital foramen (right)	0.16	0.16

(Continues)

TABLE 1 (Continued)

(Continues)

TABLE 1 (Continued)

ID	Landmark description	Contrib. to RSC1 (%)	Contrib. to RSC2 (%)
57	Anterior margin of the ventral infraorbital foramen (left)	0.19	0.14
58	Junction of the left and right maxilla with the palatine	0.43	1.34
59	Junction of vomer, right and left maxilla on the ventral side of the rostrum	1.61	0.17
60	Anterior tip of the pterygoid hamulus (right)	0.39	1.67
61	Anterior tip of the pterygoid hamulus (left)	0.40	1.87
62	Anterior tip of the palatine (right)	0.56	1.56
63	Anterior tip of the palatine (left)	0.63	1.67
A	Centroid of right mandibular condyle	0.78	3.25
B	Intersection point between the labial and buccal surface on the ventral portion	5.10	**32.01**
C	Intersection point between the labial and buccal surface on the dorsal portion	0.53	10.93
D	Anteriormost point of mandibular foramen	0.12	13.67
E	Right posterior end of alveolar groove	2.74	15.20
F	Posterior symphysis centroid	**47.58**	**18.45**
G	Anterior symphysis centroid	**42.44**	2.71
H	Posterior margin of the posteriormost mental foramina	0.71	3.78

Bolded numbers indicate higher values of contribution to RSC's.

are henceforth referred to as residual shape components (RSCs; Mitteroecker et al., 2004). Additionally, multivariate trajectory analysis was performed through a linear model evaluation with a randomized residual permutation procedure (RRPP) (*lm.rrpp* function in *RRPP* package) (Collyer & Adams, 2013, 2018). Accordingly, a vector of coefficients defines the linear change of each shape variable per unit change of size. Thus, pairwise comparisons were performed to evaluate statistical differences relative to their trajectory size (i.e., vector length), which describe how much shape change occurs per unit change of size and shape, and which describe the differences in their locations in tangent space (Collyer et al., 2015).

Three dimensional plots (i.e., html files) displaying the predicted shapes of the smallest and largest specimens from the regression scores of the linear model and the mean shape were created using the *plotRefToTarget* function (see below) to represent the post-natal development of each species. All functions used here are available in the *geomorph* package (Adams & Otárola-Castillo, 2013), except for the trajectory analysis. Please note, that all html files are recommended to be visualized in a web browser, zooming out to ensure that you see the whole frame.

2.4 | Phylogenetic approach

Since frequency and source level are, respectively, inversely and directly related to body mass in toothed whales (Jensen et al., 2018), macroevolutionary patterns in sound production of toothed whales were investigated through the comparison of species with similar body size and sound production properties. A "phylosoundspace" was created from the original phylomorphospace method (Sidlauskas, 2008) which plots the phylogenetic relationships of the species relative to two (2D) or three (3D) continuous traits. Here, the sound space for toothed whales was based on the centroid frequency (kHz, CF), source level (dB re. 1µPa, SL) (Jensen et al., 2018) and the maximum body mass (kg) (Folkens & Reeves, 2002). We used logarithmically transformed values for body mass to compare all odontocetes due to the great range in size. The phylogenetic relationship of toothed whales was based on McGowen et al. (2020). Missing values from species with no information were estimated using ancestral states reconstruction under a Brownian evolution model using the likelihood method (*anc.ML* function in *phytools* package) (Revell, 2012). The "phylosoundspace" in three dimensions was created using *phylomorphospace3d* function from the *phytools* package (Revell, 2012).

Additionally, the evolution of the feeding portion of the lower jaw (i.e., number of tooth pairs in the mandible) (Folkens & Reeves, 2002) was compared to the specific residual values from the linear models (a) CF ~log(Body mass) and (2) SL ~log(Body mass) using phylogenetic generalized least squares (PGLS, (*pgls* function in *caper* package) (Orme et al., 2013) to investigate, in general, whether the sound production of specialized feeding strategists might be

influenced by the rostrum morphology. Tooth morphology was not taken into account. All variables used in the statistical analysis are summarized in File S3.

3 | RESULTS

Prediction lines were primarily dependent on changes in the tip of the rostrum (49.06%) for the skull and both posteriormost and anteriormost point of the mandibular symphysis (90.02%) (Figure 1, Table 1). Notably, the long-narrow rostrum species *P. blainvillei* presented remarkable inclination compared to the other species, and *S. plumbea* exhibited the most inclined prediction lines between delphinids for the skull. The first RSC is also strongly influenced by the tips of the skull and mandible (Figure 2, Table 1), which segregate *P. blainvillei* considerably from the rest. On the other hand, less pronounced inclinations of prediction lines were found for both short rostrum species, *P. phocoena* and *L. albirostris* (Figure 1).

The RSCs for the skull data revealed the expected divergence for the long-rostrum *P. blainvillei*, as the tip of the rostrum variation contributed considerably to the first component (Table 1). In the same way, the long-rostrum *S. plumbea* exhibited higher values for RSC1 compared to the other delphinids (Figure 2). Predicted shapes for the smallest and largest specimen revealed that the postnatal development of the rostrum also varies relative to body axis. *P. blainvillei* not only exhibits a remarkable anterior elongation of the maxillary and premaxillary bones but also a clear ventral displacement of the tip of the rostrum (File S4), as observed for *P. phocoena* (File S5) and *L. albirostris* (File S6). *S. plumbea* seems to exhibit a straight elongation of the rostrum i.e., without vertical displacement of the rostrum (File S7). Both *Tursiops* species exhibit a slight ventral displacement of the tip of the rostrum, but *T. truncatus* seems to present a relative reduction in rostrum size compared to the mean shape and the smallest predicted shape (File S8). RSC2 distinguished *P. phocoena* and *P. blainvillei* from the other species mainly by the position of the base of the epicranial complex which is measured by the posterior tip of the right premaxillary bone (Table 1).

RSC1 for the mandible showed that the posterior and anterior symphysis centroid variation were important for distinguishing *P. blainvillei* from the other species (Figure 2). *Sousa plumbea* presented the highest values for RSC1 compared to the other delphinids. Interestingly, RSC2 for the mandible data was considerably influenced by the intersection point between the labial and buccal surface (ventral portion) and distinguished *P. blainvillei* and *P. phocoena* from the other species. The increased mandibular foramen is remarkable in the postnatal development of the intersection point between the labial and buccal surface of the mandible at the ventral margin of the mandibular foramen as it extends posteriorly in these species (*P. blainvillei*: File S10; *P. phocoena*: File S11). The remaining species do not present remarkable changes in the posterior portion of the mandible, however adult *L. albirostris* seem to present a relatively smaller mandibular foramen compared to the other delphinids (File S12).

The position of the posterior symphysis centroid developed in distinct ways between the species analyzed here. *P. blainvillei* decreases the relative size of the mandibular symphysis (i.e., length between the posterior and anterior symphysis centroid) compared to the mean and the smallest predicted shapes for the species (File S10). *Phocoena phocoena* and *Lagenorhynchus albirostris* did not present remarkable changes in the mandibular symphysis (*P. phocoena*: File S11; *L. albirostris*: File S12), however members of Delphininae exhibited notably distinct patterns. *Sousa plumbea* exhibited a more pronounced anteriorization of the tip of the mandible compared to the posterior symphysis centroid (File S13). Similarly, in both *Tursiops* species the posterior symphysis centroid developed anteriorly compared to the species mean shapes, but differed in its tip transformation. In *T. truncatus* and *T. gephyreus*, the tip is posteriorly and anteriorly positioned, respectively, compared to the species mean shapes (*T. truncatus*: File S14; *T. gephyreus*: File S15). Coincidentally, species that decreased the relative size of the lower jaw (i.e., *P. phocoena*, *L. albirostris* and *T. truncatus*) exhibited anterior displacement of the posteriormost mental foramina compared to the remaining species that presented a caudal displacement of the posteriormost trigeminal branch of the mandible.

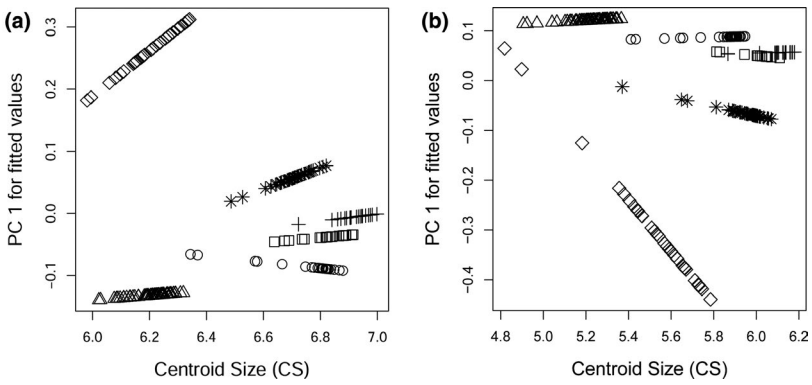

FIGURE 1 Skull and mandible variation throughout development is primarily dependent on changes in the tip of the rostrum. Prediction lines for the (a) skull and (b) mandible development based on the first principal component of "predicted" values from the linear model with centroid size (CS). Diamond, *Pontoporia blainvillei*; triangle, *Phocoena phocoena*; circle, *Lagenorhynchus albirostris*; asterisk, *Sousa plumbea*; cross, *Tursiops gephyreus*; square, *Tursiops truncatus*

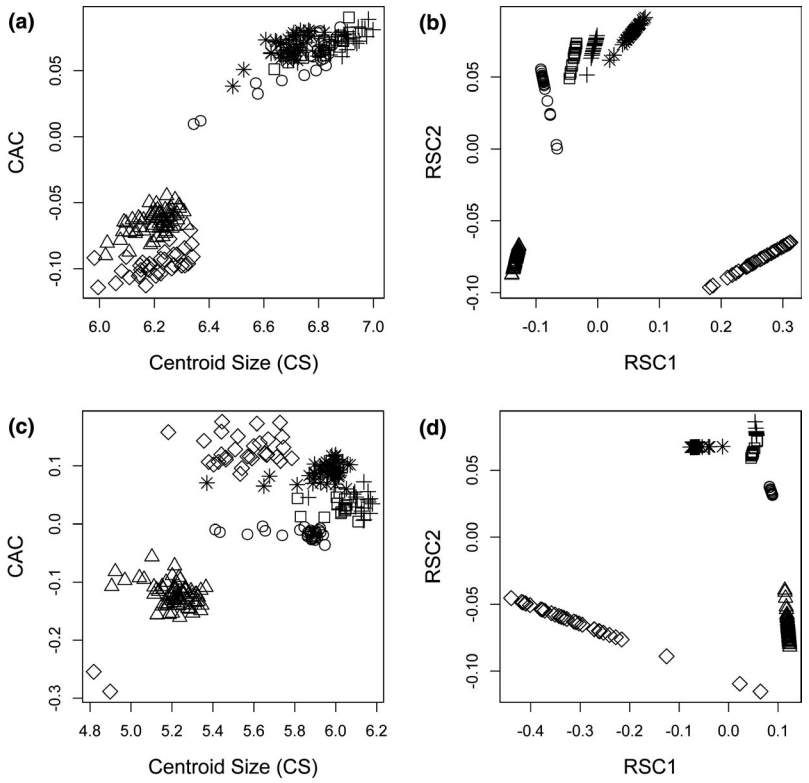

FIGURE 2 Postnatal development patterns for the skull and mandible. The common allometric component (CAC) for the (a) skull and (c) mandible data indicating the estimation of the average allometric trend for group-mean centered data. The remaining variables for the (b) skull and (d) mandible were assessed through the first and second Residual Shape Component (RSC). Diamond, *Pontoporia blainvillei*; triangle, *Phocoena phocoena*; circle, *Lagenorhynchus albirostris*; asterisk, *Sousa plumbea*; cross, *Tursiops gephyreus*; square, *Tursiops truncatus*

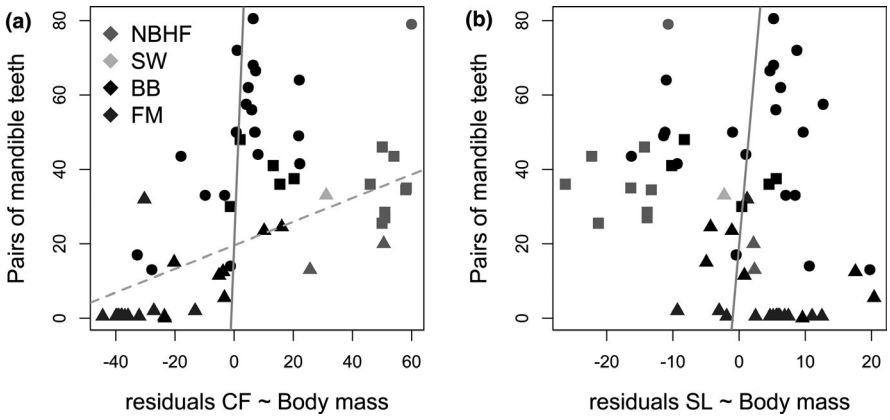

FIGURE 3 Sound production in raptorial species is linked to rostrum morphology. The number of tooth pairs in the mandible (TP) as a function of the residuals from the linear models (a) CF ~log(Body mass) and (b) SL ~log(Body mass) relative to feeding strategy using phylogenetic generalized least squares (PGLS). Colors represent species classification according to sound production parameters (Jensen et al., 2018; Zimmer et al., 2005). Dashed lines in A represent significant correlation between TP and residuals of CF ~log(Body mass) (i.e., including all toothed whales, $p = 0.012$). Continuous grey lines in a and b indicate high correlation between TA and the residuals of both linear models for raptorial species whales (PGLS A: $\lambda = 0.84$, $R^2 = 0.32$, $p < 0.01$; PGLS B: $\lambda = 0.93$, $R^2 = 0.21$, $p < 0.01$). CF, centroid frequency; SL, source level; NBHF, narrow-band high-frequency, SW, sperm whale; BB, broad-band; FM, frequency-modulated. Feeding strategy classification followed Werth (2006), Johnston and Berta (2011) and Galatius et al. (2020): octagon, raptorial; square, combination; triangle, suction

The "phylosoundspace" revealed that toothed whales evolved distinct head shapes (e.g., long and short-rostrum heads, associated with specialized feeding modes) into similar sound emission properties (e.g., *L. albirostris* and *S. chinensis*; genus *Orca* and some ziphiids, in the same way as observed for NBHF species (e.g., *P. blainvillei* and *P. phocoena*). In fact, the evolution of the anterior portion

TABLE 2 Attribute differences (*d*), standardized scores (*Z*), and *p*-values (*p*) for skull and mandible trajectories. Significant values are indicated in bold.

	Skull								Mandible							
	Trajectory shape differences				Magnitude differences in size				Trajectory shape differences				Magnitude differences in size			
Pairwise comparisons	*d*	UCL (95%)	*Z*	*p*	*d*	UCL (95%)	*Z*	*p*	*d*	UCL (95%)	*Z*	*p*	*d*	UCL (95%)	*Z*	*p*
L. albirostris: *P. phocoena*	0.03	0.02	3.15	0.015	0.00	0.01	−0.37	0.575	0.04	0.04	2.34	0.02	0.00	0.03	−0.96	0.815
L. albirostris: *P. blainvillei*	0.11	0.03	9.57	**0.005**	0.08	0.02	10.81	**0.005**	0.20	0.05	9.97	**0.005**	0.09	0.03	6.89	**0.005**
L. albirostris: *S. plumbea*	0.05	0.02	4.73	**0.005**	0.02	0.01	4.54	**0.005**	0.08	0.04	5.06	**0.005**	0.09	0.03	7.61	**0.005**
L. albirostris: *T. gephyreus*	0.04	0.03	3.25	0.01	0.02	0.01	4.02	**0.005**	0.02	0.05	0.15	0.37	0.01	0.04	−0.26	0.525
L. albirostris: *T. truncatus*	0.01	0.03	0.13	0.39	0.01	0.01	1.69	0.05	0.02	0.05	−0.22	0.47	0.02	0.04	0.88	0.185
P. phocoena: *P. blainvillei*	0.13	0.02	11.60	**0.005**	0.09	0.01	11.60	**0.005**	0.21	0.04	11.02	**0.005**	0.09	0.03	7.43	**0.005**
P. phocoena: *S. plumbea*	0.08	0.02	9.94	**0.005**	0.02	0.01	4.82	**0.005**	0.09	0.03	7.15	**0.005**	0.08	0.02	8.33	**0.005**
P. phocoena: *T. gephyreus*	0.07	0.02	7.77	**0.005**	0.02	0.01	3.87	**0.005**	0.02	0.04	−0.15	0.49	0.01	0.03	−0.53	0.655
P. phocoena: *T. truncatus*	0.04	0.02	4.80	**0.005**	0.01	0.01	1.35	0.11	0.04	0.04	1.14	0.145	0.02	0.03	0.70	0.225
P. blainvillei: *S. plumbea*	0.09	0.02	9.08	**0.005**	0.11	0.01	12.14	**0.005**	0.12	0.04	7.76	**0.005**	0.00	0.03	−0.83	0.77
P. blainvillei: *T. gephyreus*	0.09	0.03	8.55	**0.005**	0.11	0.01	11.48	**0.005**	0.21	0.05	9.04	**0.005**	0.08	0.04	4.75	**0.005**
P. blainvillei: *T. truncatus*	0.10	0.03	9.69	**0.005**	0.10	0.02	10.86	**0.005**	0.19	0.05	8.59	**0.005**	0.07	0.04	4.19	**0.005**
S. plumbea: *T. gephyreus*	0.01	0.03	−0.47	0.645	0.00	0.01	−1.18	0.91	0.08	0.05	4.38	0.01	0.07	0.03	5.57	**0.005**
S. plumbea: *T. truncatus*	0.03	0.03	2.99	0.015	0.01	0.01	0.83	0.205	0.06	0.05	2.83	0.02	0.06	0.04	4.06	**0.005**
T. gephyreus: *T. truncatus*	0.02	0.03	1.34	0.135	0.01	0.02	0.72	0.23	0.02	0.06	−0.22	0.485	0.01	0.04	−0.32	0.54

of the skull is strongly influenced by phylogeny and might not only explain the feeding mode, but also morphological adaptations for sound production in toothed whales (PGLS 1: λ = 0.84, R^2 = 0.32, p < 0.01; PGLS 2: λ = 0.93, R_2 = 0.21, p < 0.01), particularly in raptorial species (PGLS 1: slope = 14.5, p < 0.001; PGLS 2: slope = 12.7, p < 0.001) (Figure 3).

4 | DISCUSSION

Our results demonstrate that sound production might be related to rostrum morphology as the centroid frequency tends to increase together with the number of pairs of teeth in the lower jaw, especially for raptorial specialists (Figure 3). Although tooth morphology might also be determined by prey size, raptorial species exhibiting medium to enlarged teeth such as *Sotalia* and *Steno* seem to follow the same pattern (File S16). However, further investigation should address specific relations between sound parameters within raptorial species. The shape and number of tooth pairs in the mandible (and the upper jaw) seem to be set during early foetal stages as the anterior portion of the rostrum nasi cartilage differs considerably in size between e.g., the raptorial specialist *P. blainvillei* and the short-rostrum species *P. phocoena* and *L. albirostris* (Frainer et al., 2019a) which present combinations of suction and raptorial feeding (Johnston & Berta, 2011). Thus, the rostrum exhibits an increased timing of development between raptorial species and the other specialists analyzed here (Files S4–S15). In this way, rostrum transformation throughout ontogeny might be crucial to modulate specialized sounds (e.g., with higher centroid frequency and source level) in raptorial specialists, which might indicate the achievement of a more directional sound emission system compared to lineages exhibiting a purer feeding strategy.

The variation of upper and lower jaw morphology encompassed the major differences between the species analyzed here, and reflects the distinct feeding strategies adopted by these species, i.e., suction feeding, mainly for short rostrum species, raptorial feeding for species that manipulate prey before ingesting, or the combination of both for intermediate species (Werth, 2006). Head morphology of extant dolphins might have evolved under relaxed constraints on the directionality of the sound beam due to distinct heterochronic process acting on key structures involved in sound production (Frainer et al., 2019a; Haddad et al., 2012; Rauschmann et al., 2006). The increased rostrum development (Figures 1 and 2, Table 2) might reflect increasingly directional properties for raptorial species such as *P. blainvillei* and *S. plumbea* (Jensen et al., 2018; Johnston & Berta, 2011; Song et al., 2016). Thus, raptorial specialists seem to depend on the postnatal development of the rostrum to acquire the characteristic sound emission as found in adults (Frainer et al., 2015).

Suction feeding species may have evolved under paedomorphic events (Galatius, 2010) on rostrum formation as observed by the low shape differentiation throughout ontogeny in *P. phocoena* and *L. albirostris* (Figures 1 and 2, Table 2). Additionally, these species exhibited no significant differences in trajectory size and shape for both skull and mandible datasets. These shared changes during the postnatal transformation of the skull by independent lineages could indicate common selective pressures (Langerhans & DeWitt, 2004) underlying the evolution of paedomorphic species. In these species, the soft tissue structures in the epicranial complex may play a greater role in sound modulation and emission than the rostrum (Frainer et al., 2019a; Huggenberger et al., 2009; McKenna et al., 2012).

As observed for NBHF species which exhibit distinct epicranial complex morphology but similar sound emission parameters (Frainer et al., 2019a), some delphinid members seem to have evolved distinct head shapes for similar sound production such as typical long and short-rostrum species (File S16). *L. albirostris* and *S. plumbea* are similar in position within the "phylosoundspace" of toothed whales (File S16) due to similar body size and biosonar parameters (assuming similar sound production properties as in *S. chinensis*, Jensen et al., 2018). However, they presented distinct ontogenetic parameters related to skull changes (Table 2; *L. albirostris*: File S6; *S. plumbea*: File S7). As the rostrum represents one among other structures that modulate directionality in sound production for some odontocetes (Song et al., 2016), the postnatal development seems to represent a crucial stage for biosonar maturation in some raptorial species such as *P. blainvillei* and *S. plumbea* (File S1).

Although *P. blainvillei* and *P. phocoena* exhibited remarkable differences in trajectory shape and size (Table 2), both species presented similar morphology at the base of the epicranial complex (and the posterior portion of the mandible, see below; Table 2). RSC2 was strongly influenced by the position of the posterior portion of the right premaxillary bone, which is the base for the premaxillary air sacs (Mead, 1975). Although *P. phocoena* exhibits a higher vertex of the skull compared to *P. blainvillei*, the position of the posterior tip of the premaxillary bone in both species is anteroventrally extended compared to the other species. On the other hand, *Cephalorhynchus* dolphins are rather similar to broad-band delphinids in this respect. The shape of the skull might reflect the soft tissue anatomy associated with it, although soft tissue composition (e.g., branches of the melon) differ considerably among NBHF species (Frainer et al., 2019a). Frainer et al. (2019a) proposed that the horizontal alignment of the bursae complex with the posterior portion of the melon might represent one among other adaptations for the production of highly directional sounds as observed in *Cephalorhynchus*, *P. phocoena* and *P. blainvillei*. Thus, distinct trajectories of the skull shape might achieve a similar arrangement of the biosonar's soft tissue anatomy.

The clicks produced in the epicranial complex travel through the environment and the echoes of reflective objects are perceived as vibrations through the acoustic window of the lower jaw (Norris, 1968) or, in another point of view, via the gular region in *Ziphius cavirostris* (Cranford et al., 2008). The remarkable development of the mandibular foramen in both NBHF species analyzed here might, among other things, be related to their similar inner ear morphology (Galatius et al., 2019), as convergent adaptations to achieve a highly sensitive sound receiving apparatus at specific high frequencies. On the other hand, delphinids exhibit low differentiation on the mandibular foramen compared to *P. blainvillei* and *P. phocoena*, but striking

differences on the development of the mandible tip (anterior to the posterior symphysis centroid). In this vein, ontogenetic changes in the "feeding portion" of the lower jaw might independently reflect acquired transformations that regulate rostrum size in dolphins (Frainer et al., 2019a) which might be constrained by upper jaw changes throughout postnatal ontogeny.

Since the anterior "feeding portion" of the lower jaw with its tooth apparatus is not directly involved in sound reception, ontogenetic changes in the rostrum (including pre and postnatal transformations) (Frainer et al., 2019a) might have followed convergent trajectories to adhere to both the particular feeding strategy (Werth, 2006) and sound production. Alternatively, the variation in the mental foramina arrangement at the anterior portion of the mandible could reflect another mechanism of environment perception as dolphins are highly sensitive to (sound) vibrations at the tip of the lower jaw up to areas below the eye (Bullock et al., 1968; McCormick et al., 1970). Our study demonstrated that species presenting anterior development of the mandible tip compared to the mean shape and the smallest predicted shape for each species, also exhibited a posteriorization of the mental foramina. Thus, mandible development in dolphins might have evolved under similar selective pressures working on the postnatal development as in the skull, but through independent process.

Toothed whales are the most diverse group among cetaceans and all marine mammals (Rice, 2009) in which the main commonalities are the evolution of the echolocation and their complex social organization (May-Collado et al., 2007). The family Delphinidae represents the most diverse group among all marine mammals including two distinct lineages that are globally distributed and well adapted to both coastal and offshore environments: the *Tursiops* and *Orcinus* genera. In this study, we evaluated intrageneric variation by comparing ontogenies of close related coastal (i.e., *T. gephyreus*) and mostly oceanic (*T. truncatus*, in this case) lineages (see Wickert et al., 2016). Although both skull and mandible trajectories exhibited no differences in shape and size (Table 2), the variation observed in rostrum development might illustrate the shape plasticity found in the genus.

Orcas (*Orcinus orca*) also exhibit great variation in rostrum size e.g., when comparing Type A and Type D individuals (Pitman et al., 2020), although melon development may also influence this general arrangement (Frainer et al., 2019a). Nevertheless, it reflects the ecological plasticity in these groups (Foote et al., 2009) and might directly affect the directional properties of sound emission (Song et al., 2016). Combined with a complex socio-cultural development (Fox et al., 2017), these features might explain, in part, their increased success in the marine environment (Kaschner et al., 2011; Pyenson, 2017). On the other hand, suction or raptorial feeding specialists seem to present prey specific preferences (McCurry et al., 2017) which may have driven the evolution of skull morphology (Galatius et al., 2020). Thus, it would be plausible to assume distinct sound modulation strategies to hunt prey with characteristic sound reflection properties (e.g., squid vs. fish).

Coastal dolphins with highly directional sound production are limited on performing wide range adjustments while pursuing prey or avoiding obstacles (Moore et al., 2008). The late transformation of the rostrum might reflect shifts in the feeding and/or behavioural (acoustic) patterns of these species (Plön et al., 2015; Troina et al., 2016) and potentially indicate higher vulnerability when facing a changing environment. Young individuals of coastal NBHF species and *S. plumbea* (i.e., mainly male adolescents) seem to be more susceptible to die in gill nets (Atkins et al., 2013; Reeves et al., 2013) and this might be related to, among other things, the late development of an important structure to modulate biosonar clicks (i.e., rostrum) (Song et al., 2016) and their restricted field of perception compared to other coastal forms such as *T. gephyreus* (Frainer et al., 2019b).

In this study, we demonstrated that sound production may be influenced by the rostrum morphology in toothed whales, mainly for raptorial specialists that tend to present higher values of centroid frequency and source level. Thus, postnatal development seems to represent a crucial stage for biosonar maturation in some raptorial species as the rostrum exhibits remarkable transformation compared to what is seen in specialized suction feeders. The ontogeny of the biosonar structures—the main tool for navigation and hunting in toothed whales—might reflect their natural history peculiarities and thus potentially define their main threats.

ACKNOWLEDGMENTS

Our special thanks to Dr. Greg Hofmeyr (Port Elizabeth Museum at Bayworld), Daniel Klingberg Johansson (Natural History Museum of Copenhagen – NHMC), and Dr. Janaína Wickert (Natural Sciences Museum of the Federal University of Rio Grande do Sul – MUCIN/UFRGS, and Grupo de Estudos de Mamíferos Aquáticos do Rio Grande do Sul – GEMARS) for their assistance during the "field" work at the museums. A special thanks to Dr. Rachel Racicot and an anonymous reviewer for their comments and suggestions. A great thanks to Alexandra Elbakyan (sci-hub) for providing access of most information contained here. A great thanks to the geomorph community for their logistical support. G.F. was supported by a PhD scholarship from Coordenação de Aperfeiçoamento de Pessoal de Nível Superior (CAPES) (from 2015 to 2019) and Conselho Nacional de Desenvolvimento Científico e Tecnológico (CNPq) (Ciências Sem Fronteiras – grant number 201709/2015-5). This study was only possible due to the financial support from small grants in aid of research (year 2016) provided by the Society for Marine Mammalogy (U.S.). This is a contribution of the Research Group "Evolução e Biodiversidade de Cetáceos/CNPq".

AUTHOR CONTRIBUTIONS

GF, SF, IM and AG all contributed to the conception and design of the study and interpretation of the data. GF acquired the three dimensional landmarks for each specimen and performed the statistical analysis under AG's assistance. GF drafted the manuscript and SF, IM and AG revised it critically. All authors gave final approval before submission.

DATA AVAILABILITY STATEMENT

The data that support the findings of this study are available from the corresponding author upon reasonable request.

ORCID

Guilherme Frainer https://orcid.org/0000-0002-5527-9219
Stefan Huggenberger https://orcid.org/0000-0002-8085-5927
Ignacio B. Moreno https://orcid.org/0000-0001-9854-6033
Anders Galatius https://orcid.org/0000-0003-1237-2066

REFERENCES

Adams, D.C. & Nistri, A. (2010) Ontogenetic convergence and evolution of foot morphology in European cave salamanders (Family: Plethodontidae). *BMC Evolutionary Biology*, 10, 216.

Adams, D.C. & Otárola-Castillo, E. (2013) geomorph: An r package for the collection and analysis of geometric morphometric shape data. *Methods in Ecology and Evolution*, 4, 393–399.

Atkins, S., Cliff, G. & Pillay, N. (2013) Humpback dolphin bycatch in the shark nets in KwaZulu-Natal, South Africa. *Biological Conservation*, 159, 442–449.

Au, W.L. (2000) Hearing in whales and dolphins: An overview. In: Au, W.L. and Richard, R.F. (Eds.) *Hearing by whales and dolphins*. New York: Springer, pp. 1–42.

Barroso, C., Cranford, T.W. & Berta, A. (2012) Shape analysis of odontocete mandibles: Functional and evolutionary implications. *Journal of Morphology*, 273, 1021–1030.

Bookstein, F.L. (1991) *Morphometric tools for landmark data: Geometry and biology*. Cambridge: Cambridge University Press.

Bullock, T., Grinnell, A., Ikezono, E. et al. (1968) Electrophysiological studies of central auditory mechanisms in cetaceans. *Journal of Comparative Physiology A: Neuroethology, Sensory, Neural, and Behavioral Physiology*, 59, 117–156.

Collyer, M.L. & Adams, D.C. (2013) Phenotypic trajectory analysis: Comparison of shape change patterns in evolution and ecology. *Hystrix, the Italian Journal of Mammalogy*, 24, 75–83.

Collyer, M.L. & Adams, D.C. (2018) RRPP: An r package for fitting linear models to high-dimensional data using residual randomization. *Methods in Ecology and Evolution*, 9, 1772–1779.

Collyer, M.L., Sekora, D.J. & Adams, D.C. (2015) A method for analysis of phenotypic change for phenotypes described by high-dimensional data. *Heredity*, 115, 357–365.

Cranford, T.W., McKenna, M.F., Soldevilla, M.S., Wiggins, S.M., Goldbogen, J.A., Shadwick, R.E., Krysl, P. et al. (2008) Anatomic geometry of sound transmission and reception in Cuvier's Beaked Whale (*Ziphius cavirostris*). *The Anatomical Record*, 291, 353–378.

Finneran, J.J., Branstetter, B.K., Houser, D.S. et al. (2014) High-resolution measurement of a bottlenose dolphin's (*Tursiops truncatus*) biosonar transmission beam pattern in the horizontal plane. *The Journal of the Acoustical Society of America*, 136, 2025–2038.

Fish, F.E. (2002) Balancing requirements for stability and maneuverability in Cetaceans. *Integrative and Comparative Biology*, 42, 85–93.

Folkens, P.A. & Reeves, R.R. (2002) *Guide to marine mammals of the world*. New York: National Audubon Society.

Foote, A.D., Newton, J., Piertney, S.B., Willerslev, E. & Gilbert, M.T.P. (2009) Ecological, morphological and genetic divergence of sympatric North Atlantic killer whale populations. *Molecular Ecology*, 18, 5207–5217.

Fox, K.C.R., Muthukrishna, M. & Shultz, S. (2017) The social and cultural roots of whale and dolphin brains. *Nature Ecology & Evolution*, 1, 1699–1705.

Frainer, G., Huggenberger, S. & Moreno, I.B. (2015) Postnatal development of franciscana's (*Pontoporia blainvillei*) biosonar relevant structures with potential implications for function, life history, and bycatch. *Marine Mammal Science*, 31, 1193–1212.

Frainer, G., Moreno, I.B., Serpa, N., Galatius, A., Wiedermann, D. & Huggenberger, S. (2019a) Ontogeny and evolution of the sound-generating structures in the infraorder Delphinida (Odontoceti: Delphinida). *Biological Journal of the Linnean Society*, 128(3), 700–724.

Frainer, G., Plön, S., Serpa, N.B., Moreno, I.B. & Huggenberger, S. (2019b) Sound generating structures of the Humpback Dolphin *Sousa plumbea* (Cuvier, 1829) and the directionality in dolphin sounds. *The Anatomical Record*, 302, 849–860.

Galatius, A. (2010) Paedomorphosis in two small species of toothed whales (Odontoceti): How and why? *Biological Journal of the Linnean Society*, 99, 278–295.

Galatius, A. & Gol'din, P.E.(2011) Geographic variation of skeletal ontogeny and skull shape in the harbour porpoise (*Phocoena phocoena*). *Canadian Journal of Zoology*, 89, 869–879.

Galatius, A. & Goodall, N.P. (2016) Skull shapes of the Lissodelphininae: Radiation, adaptation and asymmetry. *Journal of Morphology*, 277, 776–785.

Galatius, A., Olsen, M.T., Steeman, M.E. Racicot, R.A., Bradshaw, C.D., Kyhn, L.A. et al. (2019) Raising your voice: evolution of narrow-band high-frequency signals in toothed whales (Odontoceti). *Biological Journal of the Linnean Society*, 126, 213–224.

Galatius, A., Racicot, R.A., McGowen, M.R. & Olsen, M.T. (2020) Evolution and diversification of delphinid skull shapes. *IScience*, 23, 101543.

Geisler, J.H., Colbert, M.W. & Carew, J.L. (2014) A new fossil species supports an early origin for toothed whale echolocation. *Nature*, 508, 383.

Gunz, P., Mitteroecker, P., Neubauer, S., Weber, G.W. & Bookstein, F.L. (2009) Principles for the virtual reconstruction of hominin crania. *Journal of Human Evolution*, 57, 48–62.

Haddad, D., Huggenberger, S., Haas-Rioth, M., Kossatz, L.S., Oelschläger, H.H.A. & Haase, A. (2012) Magnetic resonance microscopy of prenatal dolphins (Mammalia, Odontoceti, Delphinidae) – Ontogenetic and phylogenetic implications. *Zoologischer Anzeiger – A Journal of Comparative Zoology*, 251, 115–130.

Huggenberger, S., Rauschmann, M.A., Vogl, T.J. & Oelschläger, H.H.A. (2009) Functional morphology of the nasal complex in the harbor porpoise (*Phocoena phocoena* L.). *The Anatomical Record*, 292, 902–920.

Jensen, F.H., Bejder, L., Wahlberg, M. & Madsen, P.T. (2009) Biosonar adjustments to target range of echolocating bottlenose dolphins (*Tursiops* sp.) in the wild. *Journal of Experimental Biology*, 212, 1078.

Jensen, F.H., Johnson, M., Ladegaard, M., Wisniewska, D.M. & Madsen, P.T. (2018) Narrow acoustic field of view drives frequency scaling in toothed whale biosonar. *Current Biology*, 28, 3878–3885.e3.

Johnston, C. & Berta, A. (2011) Comparative anatomy and evolutionary history of suction feeding in cetaceans. *Marine Mammal Science*, 27, 493–513.

Kaschner, K., Tittensor, D.P., Ready, J., Gerrodette, T. & Worm, B. (2011) Current and future patterns of global marine mammal biodiversity. *PLoS One*, 6, e19653.

Koblitz, J.C., Wahlberg, M., Stilz, P., Madsen, P.T., Beedholm, K. & Schnitzler, H.U. (2012) Asymmetry and dynamics of a narrow sonar beam in an echolocating harbor porpoise. *The Journal of the Acoustical Society of America*, 131, 2315–2324.

Kyhn, L.A., Jensen, F.H., Beedholm, K., Tougaard, J., Hansen, M. & Madsen, P.T. (2010) Echolocation in sympatric Peale's dolphins (*Lagenorhynchus australis*) and Commerson's dolphins (*Cephalorhynchus commersonii*) producing narrow-band high-frequency clicks. *The Journal of Experimental Biology*, 213, 1940.

Langerhans, R.B. & DeWitt, T.J. (2004) Shared and unique features of evolutionary diversification. *The American Naturalist*, 164, 335–349.

Madsen, P.T., Lammers, M.O., Wisniewska, D. & Beedholm, K. (2013) Nasal sound production in echolocating delphinids (*Tursiops truncatus* and *Pseudorca crassidens*) is dynamic, but unilateral: Clicking on the right side and whistling on the left side. *Journal of Experimental Biology*, 216, 4091–4102.

May-Collado, L.J., Agnarsson, I. & Wartzok, D. (2007) Phylogenetic review of tonal sound production in whales in relation to sociality. *BMC Evolutionary Biology*, 7, 136.

McCormick, J.G., Wever, E.G., Palin, J. & Ridgway, S.H. (1970) Sound conduction in the dolphin ear. *The Journal of the Acoustical Society of America*, 48, 1418–1428.

McCurry, M.R., Fitzgerald, E.M.G., Evans, A.R., Adams, J.W. & McHenry, C.R. (2017) Skull shape reflects prey size niche in toothed whales. *Biological Journal of the Linnean Society*, 121, 936–946.

McGowen, M.R., Tsagkogeorga, G., Álvarez-Carretero, S., dos Reis, M., Struebig, M., Deaville, R. et al. (2020) Phylogenomic resolution of the Cetacean tree of life using target sequence capture. *Systematic Biology*, *69*, 479–501.

McKenna, M.F., Cranford, T.W., Berta, A. & Pyenson, N.D. (2012) Morphology of the odontocete melon and its implications for acoustic function. *Marine Mammal Science*, 28, 690–713.

Mead, J.G. (1975) Anatomy of the external nasal passages and facial complex in the Delphinidae (Mammalia: Cetacea). *Smithsonian Contributions to Zoology*, 207, 1–35.

Mead, J.G. & Fordyce, R.E. (2009) The Therian skull: A lexicon with emphasis on the odontocetes. *Smithsonian Contributions to Zoology*, 627, 1–249.

Mitteroecker, P., Gunz, P., Bernhard, M., Schaefer, K. & Bookstein, F.L. (2004) Comparison of cranial ontogenetic trajectories among great apes and humans. *Journal of Human Evolution*, 46, 679–698.

Moore, P.W., Dankiewicz, L.A. & Houser, D.S. (2008) Beamwidth control and angular target detection in an echolocating bottlenose dolphin (*Tursiops truncatus*). *The Journal of the Acoustical Society of America*, 124, 3324–3332.

Norris, K. (1968) The evolution of acoustic mechanisms in odontocete cetaceans. In: Drake, E. T. (Ed.), *Evolution and Environment*. New Haven: Yale University Press, pp 297–324.

Norris, K.S., Prescott, J.H., Asa-Dorian, P.V. & Perkins, P. (1961) An experimental demonstration of echolocation behavior in the porpoise, *Tursiops truncatus* (Montagu). *The Biological Bulletin*, 120, 163–176.

Orme, D., Freckleton, R., Thomas, G., Petzoldt, T. & Fritz, S. (2013) The caper package: comparative analysis of phylogenetics and evolution in R. R package version, 5, 1–36.

Pitman, R.L., Ballance, L.T., Sironi, M., Totterdell, J., Towers, J.R. & Wellard, R. (2020) Enigmatic megafauna: type D killer whale in the Southern Ocean. *Ecology*, 101, e02871.

Plön, S., Cockcroft, V.G. & Froneman, W.P. (2015) The natural history and conservation of Indian Ocean humpback dolphins (*Sousa plumbea*) in South African waters. In: Jefferson, T.A. and Curry, B.E. (Eds.) *Advances in marine biology*. Oxford: Academic Press, pp. 143–162.

Pyenson, N.D. (2017) The ecological rise of whales chronicled by the fossil record. *Current Biology*, 27, R558–R564.

Rauschmann, M.A., Huggenberger, S., Kossatz, L.S. & Oelschläger, H.H.A. (2006) Head morphology in perinatal dolphins: A window into phylogeny and ontogeny. *Journal of Morphology*, 267, 1295–1315.

Reeves, R.R., McClellan, K. & Werner, T.B. (2013) Marine mammal bycatch in gillnet and other entangling net fisheries, 1990 to 2011. *Endangered Species Research*, 20, 71–97.

Revell, L.J. (2012) phytools: an R package for phylogenetic comparative biology (and other things). *Methods in Ecology and Evolution*, 3, 217–223.

Rice, D.W. (2009) Classification (overall). In: Perrin, W.F., Wursig, B. & Thewisse, J.G.M.(Eds.) *Encyclopedia of marine mammals*. Academic Press, pp. 234–238.

Ridgway, S.H., Dibble, D.S., Alstyne, V.K. & Price, D. (2015) On doing two things at once: dolphin brain and nose coordinate sonar clicks, buzzes and emotional squeals with social sounds during fish capture. *The Journal of Experimental Biology*, 218, 3987.

Rohlf, F.J. & Slice, D. (1990) Extensions of the procrustes method for the optimal superimposition of landmarks. *Systematic Biology*, 39, 40–59.

Sidlauskas, B. (2008) Continuous and arrested morphological diversification in sister clades of characiform fishes: A phylomorphospace approach. *Evolution*, 62, 3135–3156.

Song, Z., Zhang, Y., Wei, C. & Wang, X. (2016) Inducing rostrum interfacial waves by fluid-solid coupling in a Chinese river dolphin (*Lipotes vexillifer*). *Physical Review E*, 93, 012411.

Team (2020) *R: A language and environment for statistical computing*. Vienna, Austria: R Foundation for Statistical Computing Retrieved from http://www.r-project.org/

Thewissen, J.G.M., Cohn, M.J., Stevens, L.S., Bajpai, S., Heyning, J. & Horton, W.E. (2006) Developmental basis for hind-limb loss in dolphins and origin of the cetacean bodyplan. *Proceedings of the National Academy of Sciences*, 103, 8414.

Troina, G., Botta, S., Secchi, E.R. & Dehairs, F. (2016) Ontogenetic and sexual characterization of the feeding habits of franciscanas, *Pontoporia blainvillei*, based on tooth dentin carbon and nitrogen stable isotopes. *Marine Mammal Science*, 32, 1115–1137.

Wei, C., Au, W.W.L., Ketten, D.R., Song, Z. & Zhang, Y. (2017) Biosonar signal propagation in the harbor porpoise's (*Phocoena phocoena*) head: The role of various structures in the formation of the vertical beam. *The Journal of the Acoustical Society of America*, 141, 4179–4187.

Wei, C., Au, W.W.L., Ketten, D.R., Vishnu, H. & Ho, A.Z.H. (2019) Sound propagation in the near and far-field of a broadband echolocating dolphin and a narrowband echolocating porpoise. *Proceedings of Meetings on Acoustics*, 37, 010003.

Werth, A.J. (2006) Mandibular and dental variation and the evolution of suction feeding in odontoceti. *Journal of Mammalogy*, 87, 579–588.

Wickert, J.C., von Eye, S.M., Oliveira, L.R. & Moreno, I.B. (2016) Revalidation of *Tursiops gephyreus* Lahille, 1908 (Cetartiodactyla: Delphinidae) from the southwestern Atlantic Ocean. *Journal of Mammalogy*, 97, 1728–1737.

Zimmer, W.M.X., Johnson, M.P., Madsen, P.T. & Tyack, P.L. (2005) Echolocation clicks of free-ranging Cuvier's beaked whales (*Ziphius cavirostris*). *The Journal of the Acoustical Society of America*, 117, 3919–3927.

SUPPORTING INFORMATION

Additional supporting information may be found online in the Supporting Information section.

How to cite this article: Frainer G, Huggenberger S, Moreno IB, Galatius A. Head adaptation for sound production and feeding strategy in dolphins (Odontoceti: Delphinida). *J Anat*. 2020;00:1–12. https://doi.org/10.1111/joa.13364